IEEE Photonics Journal
An IEEE Photonics Society Publication

Open Access

Lommel-Gaussian Pulsed Beams Carrying Orbital Angular Momentum Propagation in Asymmetric Oceanic Turbulence

Volume 12, Number 1, February 2020

Ye Li
Yixin Zhang
Yun Zhu

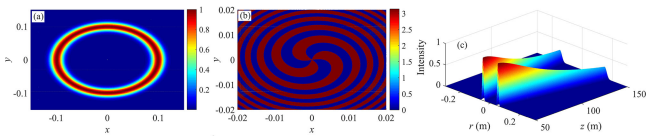

DOI: 10.1109/JPHOT.2020.2968190

Lommel-Gaussian Pulsed Beams Carrying Orbital Angular Momentum Propagation in Asymmetric Oceanic Turbulence

Ye Li,[1] **Yixin Zhang**,[1,2] **and Yun Zhu**[2]

[1]College of Internet of Things, Jiangnan University, Wuxi, Jiangsu 214000, China
[2]College of science, Jiangnan University, Wuxi, Jiangsu 214000, China

DOI:10.1109/JPHOT.2020.2968190

Manuscript received November 5, 2019; revised January 13, 2020; accepted January 16, 2020. Date of publication January 22, 2020; date of current version February 24, 2020. This work was supported by the National Natural Science Foundation of China under Grants 61871202 and 61701196.
Corresponding authors: Yixin Zhang; Yun Zhu (e-mail: zyx@jiangnan.edu.cn; zhuyun1210@163.com).

Abstract: By developing the complex phase perturbation for vortex pulsed beams in asymmetric oceanic turbulence and the spatiotemporal orthogonal basis for Lommel-Gaussian pulsed beam, we establish the received probability model of orbital angular momentum (OAM) modes for vortex pulsed beams propagating through asymmetric oceanic turbulence. Using this new model, we investigate the received probability and the pulse broadening of OAM modes of Lommel-Gaussian pulsed beam in asymmetric oceanic turbulence. Numerical simulation results show that Lommel-Gaussian pulsed beam causes a smaller pulse broadening when it propagates through oceanic turbulence with higher asymmetric factor, lower temperature structure constant, smaller inner scale and outer scale. In addition, Lommel-Gaussian pulsed beam with lower carrier frequency propagates through the oceanic turbulence with higher asymmetric factor, larger inner scale, smaller outer scale and smaller temperature structure constant, which obtains a higher received probability of signal OAM modes. For Lommel-Gaussian pulsed beams, the change of OAM quantum number has a week effect on the pulse broadening and the received probability.

Index Terms: Received probability, asymmetric oceanic turbulence, underwater wireless optical communication, ultrafast pulse, orbital angular momentum (OAM).

1. Introduction

Underwater wireless optical communication (UWOC) systems have attracted much attention due to the high anti-interference, security, bandwidth, and low cost [1]–[7], especially optical vortex beams carrying orbital angular momentum (OAM) propagating in oceanic media. Because OAM modes can form an infinite basis set to realize arbitrary base-N quantum digits that add a new degree of freedom for information coding [8]–[13]. However, oceanic turbulence causes the attenuation and the wavefront distortion of propagation beam [14]–[18]. Since the OAM is associated with the spatial distribution of the wavefunction, oceanic turbulence also distorts OAM modes of vortex beams and induces modal crosstalk among OAM channels. Some optical beams have well-defined vortices carrying OAM which can effectively mitigate the turbulent interference on these beams propagation, such as Bessel-Gaussian beam [19, 20], Hankel-Bessel beam [21], Airy beam [22], and Laguerre-Gaussian beam [23]. Recently Kovalev *et al.* [24] proposed a new type of vortex

beam called Lommel beam. This beam owns adjustable symmetry of transverse intensity pattern and continuously variable OAM, which has the better immunity to turbulent interference [25].

Small-scale self-focusing is one of the main factors that limit the system performance and efficiency of high-power laser propagation. With the rapid development of inertial confinement fusion laser communication technology, the pulsed beam is gradually applied to high power laser system due to its own advantages. To realize the high-bandwidth propagation with high frequency and data rate in wireless optical communication, the propagation of optical pulse has attracted great interest [26]–[31]. However, the temporal broadening of optical pulse caused by oceanic turbulence reduces the carried information capacity in the same situation, which restricts the performance of UWOC. Therefore, some investigations have been reported [32]–[38], which uses the vortex pulsed beam to decrease pulse broadening caused by turbulence. In the focal plane, the spatial pulse shaping of Laguerre-Gaussian pulsed beams was analyzed by Martínez-Matos *et al.* [33], which revealed the topological charge drastically jumping with evolving the pulse in time. In free space, Nie *et al.* [32] studied the spatiotemporal coupling characteristics and the intensity distribution variations of ultrashort Gaussian vortex pulse, and found that the topological charge number of the beam will affect the intensity and the spatiotemporal coupling. Liu and Gao [34] investigated the time-varying for the Laguerre-Gaussian pulsed beam propagation in the absence of turbulence, and found that a greater pulse delay and spread within short transmission distance can be caused by a higher angular quantum number. In atmospheric turbulence, the stronger refractive turbulence strength and the narrower pulse duration caused a larger scintillation of broadband pulsed Laguerre–Gaussian beams [35]. Based on the extended Huygens-Fresnel integral, Ye *et al.* [36] set up a model of the average intensity of the rotating elliptical chirped Gaussian vortex beam propagation through the isotropic oceanic turbulence. Our previous investigation for the influence of oceanic turbulence on Laguerre-Gaussian pulsed beam and Gaussian pulsed X wave revealed that the pulsed vortex beams can enhance the capacity of the oceanic turbulence link [37], [38]. In addition, Andrews *et al.* [26] showed that the outer scale of turbulence is an important parameter which affects the temporal broadening and scintillation of a beam. However, to the best of our knowledge, the effects of outer scale of asymmetric oceanic turbulence on the temporal broadening and the probability distribution function of OAM modes of the Lommel-Gaussian pulsed beam have not been reported.

In this paper, we investigate the probability distribution of OAM modes for Lommel-Gaussian pulsed beams in asymmetric oceanic turbulence based on the new pulsed OAM eigenfunctions. To study oceanic turbulence effects on the probability distribution of Lommel-Gaussian pulsed beams propagation, we develop the coherence function of Lommel-Gaussian pulsed beams in asymmetric oceanic turbulence based on the new oceanic spectrum with outer scale [39]. In addition, the new analytical expression of complex phase perturbation of spatiotemporal wave is derived. Finally, we analyze the influence of oceanic turbulence and light source parameters on the pulse broadening and the probability distribution of OAM modes of Lommel-Gaussian pulsed beams.

2. Mutual Coherence Function of Lommel-Gaussian Pulsed Beams in Oceanic Turbulence

To investigate the effects of oceanic turbulence on the Lommel-Gaussian pulsed beams carrying OAM, we start from the monochrome Lommel-Gaussian beam. In cylindrical coordinates (r, φ, z), the light field of the monochrome Lommel-Gaussian beams in the transmitter plane $(z = 0)$ can be given by [24], [25]:

$$E_n^{m_0}(r, \varphi, 0; \omega, \omega_0) = Q_1^{-m_0} \exp\left(-\frac{r^2}{w_0^2}\right) U_{m_0}\left[\frac{(\omega+\omega_0)\, r}{c \sin^{-1}(\vartheta_0)} Q_1 \exp(\mathrm{i}\varphi),\ \frac{(\omega+\omega_0)\, r}{c \sin^{-1}(\vartheta_0)}\right], \tag{1}$$

where $U_{m_0}(w, \varsigma) = \sum_{n=0}^{\infty}(-1)^n (w/\varsigma)^{m_0+2n} J_{m_0+2n}(\varsigma)$ is the Lommel function of two variables, z is the propagation distance, $J_m(\cdot)$ is the Bessel function of the first kind, $r = |r|$, $r = (x, y)$ is the two-dimensional position vector in the source plane, m_0 is OAM quantum number, φ is the azimuthal

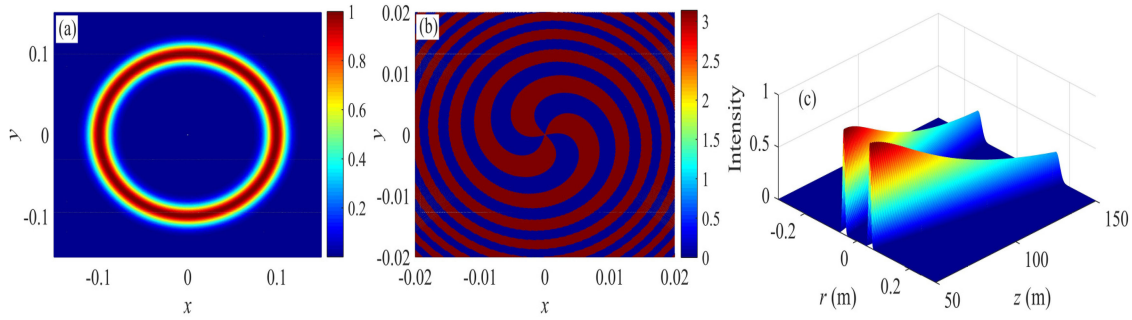

Fig. 1. (a) Radial intensity, (b) phase map, (c) transmission intensity of Lommel-Gaussian beams beam containing $m_0 = 3$ propagating from 50 m to 150 m.

angle, w_0 is the initial beam radius, Q_1 is the asymmetry parameter of beam, c is the speed of light, ϑ_0 is the Bessel cone angle, ω_0 is the signal carrier frequency, ω is the frequency.

Using the Rytov method, the field of the monochrome Lommel-Gaussian beams propagating in weak oceanic turbulence at the receiver plane can be written by [24], [40]:

$$v\left(r,\varphi,z;\omega,\omega_0\right) = E_n^{m_0}\left(r,\varphi,z;\omega,\omega_0\right)\exp\left[\psi\left(r,\varphi,z,\omega,\omega_0\right)\right], \tag{2}$$

where $\psi(r,\varphi,z,\omega,\omega_0)$ is the complex phase distortion caused by oceanic turbulence, $E_n^{m_0}(r,\varphi,z;\omega,\omega_0)$ is the monochrome scalar field of continuous Lommel-Gaussian beams in the absence of turbulence and is given by

$$E_n^{m_0}\left(r,\varphi,z;\omega,\omega_0\right) = \frac{\mathrm{i}E_0 w_0^2}{2zcQ_1^{m_0}}\exp\left[\frac{\mathrm{i}\left(\omega_0+\omega\right)}{c}\left(z+\frac{r^2}{2z}\right)-\frac{\left(\omega_0+\omega\right)^2 w_0^2}{4c^2\left(1-\mathrm{i}z_\xi\right)}\left(\sin^2\left(\vartheta_0\right)+\frac{r^2}{z^2}\right)\right]$$
$$\times\frac{\left(\omega_0+\omega\right)}{\sqrt{1+z_\xi^2}}\exp\left[\mathrm{i}\arctan\left(z_\xi\right)\right]U_{m_0}\left(\frac{\mathrm{i}\left(\omega_0+\omega\right)^2\sin\left(\vartheta_0\right)rQ_1}{2zc^2\left(1-\mathrm{i}z_\xi\right)w_0^{-2}\exp\left(-\mathrm{i}\varphi\right)},\frac{\mathrm{i}\left(\omega_0+\omega\right)^2\sin\left(\vartheta_0\right)r}{2zc^2\left(1-\mathrm{i}z_\xi\right)w_0^{-2}}\right), \tag{3}$$

where $z_\xi = z_R/z$ is the non-dimensional coordinate, $z_R = (\omega+\omega_0)w_0^2/(2c)$ is Rayleigh range, and E_0 is a constant.

In order to study the transmission characteristics of Lommel-Gaussian beams in oceanic turbulence, the light intensity and phase distribution of Lommel-Gaussian beams in Fig. 1(a) and Fig. 1(b), as well as, the attenuation law of light intensity of Lommel-Gaussian beams with the increasing of transmission distance in Fig. 1(c).

We know that the temporal properties of the pulse beam are originated from the coherence function. To investigate the coherence bandwidth of Lommel-Gaussian pulsed beams in oceanic turbulence, we use the mutual coherence function (MCF) of the complex envelope of the output Lommel-Gaussian pulsed beams by the ensemble average [28], [38], [40]

$$\left\langle W\left(r,\varphi,\varphi',z;t\right)\right\rangle = \int\int_{-\infty}^{+\infty}\frac{\exp\left[-\mathrm{i}\left(\omega-\omega'\right)t\right]}{4\pi^2}S\left(\omega\right)S^*\left(\omega'\right)\Gamma_2\left(r,\varphi,\varphi',z;\omega,\omega',\omega_0\right)\mathrm{d}\omega\mathrm{d}\omega', \tag{4}$$

where $S(\omega) = \sqrt{\pi}T_0\exp(-\omega^2T_0^2/4)$ represents the Fourier transform of the amplitude of the Gaussian pulse, T_0 is the half-pulse width of the input pulse, $\langle\cdots\rangle$ denotes the ensemble average of oceanic turbulence, and $\Gamma_2(r,\varphi,\varphi',z;\omega,\omega',\omega_0)$ is the two-frequency MCF of Lommel-Gaussian beams with OAM propagation through oceanic turbulence, and is defined as follows

$$\Gamma_2\left(r,\varphi,\varphi',z;\omega,\omega',\omega_0\right) = \Gamma_2^0\left(r,\varphi,\varphi',z;\omega,\omega'\right)\left\langle\exp\left[\psi\left(r,\varphi,z,\omega,\omega_0\right)+\psi^*\left(r,\varphi',z,\omega',\omega_0\right)\right]\right\rangle, \tag{5}$$

where $\Gamma_2^0(r,\varphi,\varphi',z;\omega,\omega') = \langle E_n^{m_0}(r,\varphi,z;\omega,\omega_0)E_n^{m_0*}(r,\varphi',z;\omega',\omega_0)\rangle$ is the two-frequency MCF of the Lommel-Gaussian beam in the absence of turbulence.

3. Complex Phase Perturbation of Spatiotemporal Wave

The theory developed thus far has described optical turbulence in the terms of spatial statistics. However, in many applications, turbulence affects the temporal properties of pulsed beams propagation. For previous studies, we structured a complex phase perturbation of spatiotemporal wave in oceanic turbulence [37], [38], which didn't consider the effects of the outer scale and asymmetric factors of oceanic turbulence. But the influence of the outer scale on the pulse width and scintillation cannot be ignored [26]. Here, we wish to set up a new complex phase perturbation of spatiotemporal waves with the outer scale of oceanic turbulence based on the spatial power spectrum of refraction-index fluctuations of asymmetric oceanic turbulence. In the following study, we consider these effects by making use of the ensemble averages of the first-order and second-order complex phase perturbation of the optical field [40]. The complex phase perturbation of vortex pulsed beams caused by asymmetric oceanic turbulence with outer scale can be given as

$$\left\langle \exp\left[\psi^*\left(r,\varphi',z;\omega',\omega_0\right)+\psi\left(r,\varphi,z;\omega,\omega_0\right)\right]\right\rangle = \exp\left[2E_1\left(0,0,0,z;\omega',\omega\right)+E_2\left(r,\varphi',\varphi,z;\omega',\omega\right)\right], \tag{6}$$

where

$$E_1\left(0,0,0,z;\omega',\omega\right) = -\frac{\pi^2 z}{c^2}\left[\left(\omega'+\omega_0\right)^2+\left(\omega+\omega_0\right)^2\right]\int_0^\infty \kappa\phi_{oc}\left(\kappa\right)\mathrm{d}\kappa, \tag{7}$$

$$E_2\left(r,\varphi,\varphi',z;\omega',\omega\right) = \frac{4\pi^2 z}{c^2}\left(\omega'+\omega_0\right)\left(\omega+\omega_0\right)\int_0^1\int_0^\infty \kappa\phi_{oc}\left(\kappa\right)J_0\left(\kappa\left|\gamma_1\vec{r}_1-\gamma_2^*\vec{r}_2\right|\right) \times \exp\left[-\frac{\mathrm{i}z\kappa^2\xi c}{2}\left(\frac{\gamma_1}{\omega+\omega_0}-\frac{\gamma_2^*}{\omega'+\omega_0}\right)\right]\mathrm{d}\kappa\mathrm{d}\xi, \tag{8}$$

where κ is the spatial wave number of turbulent fluctuations, $\vec{r}_1=(r,\varphi)$ and $\vec{r}_2=(r,\varphi')$ are the position vector, and

$$\gamma_1 = 1-\xi\left(1-\left[1-\frac{z}{F_0}-\frac{\mathrm{i}2zcw_0^{-2}}{\left(\omega+\omega_0\right)}\right]\Big/\left\{\left(1-\frac{z}{F_0}\right)^2+\left[\frac{2zcw_0^{-2}}{\left(\omega+\omega_0\right)}\right]^2\right\}\right),$$

$$\gamma_2^* = 1-\xi\left(1-\left[1-\frac{z}{F_0}+\frac{\mathrm{i}2zcw_0^{-2}}{\left(\omega'+\omega_0\right)}\right]\Big/\left\{\left(1-\frac{z}{F_0}\right)^2+\left[\frac{2zcw_0^{-2}}{\left(\omega'+\omega_0\right)}\right]^2\right\}\right), \tag{9}$$

where F_0 denotes the phase front radius of curvature of the beam wave at the transmitter.

Because of the large attenuation of optical signals caused by seawater [18], the propagation distance of optical signal in seawater is limited to 200 m. Therefore, as the wavelength of signal in the seawater "window" region, we can take the approximation $2zc/[(\omega'+\omega_0)w_0^2] \ll 1$. For the collimated beam ($F_0 \approx \infty$), γ_1 and γ_2^* in Eq. (9) can be approximated as

$$\gamma_1 \cong 1, \quad \gamma_2^* \cong 1. \tag{10}$$

The approximate expression of the Eq. (8) by the above results in Eq. (10) can be obtained as

$$E_2\left(r,\varphi,\varphi',z;\omega',\omega\right) = \frac{4\pi^2 z}{c^2}\left(\omega'+\omega_0\right)\left(\omega+\omega_0\right)\int_0^1\int_0^\infty \kappa\phi_{oc}\left(\kappa\right)J_0\left[\kappa r\sqrt{2-2\cos\left(\varphi-\varphi'\right)}\right] \times \exp\left[-\frac{\mathrm{i}z\kappa^2\xi c\left(\omega'-\omega\right)}{2\left(\omega+\omega_0\right)\left(\omega'+\omega_0\right)}\right]\mathrm{d}\kappa\mathrm{d}\xi. \tag{11}$$

Although the short pulses are ordinarily classified as wideband, the transmitted waveform may still be considered narrowband. Further, under the narrowband assumption ($(\omega-\omega') \ll \omega_0$) and

the paraxial approximation [41] ($J_0(x) \approx 1 - x^2/4$), the Eq. (6) is simplified as

$$\left\langle \exp\left[\psi^*\left(r, \varphi', z; \omega', \omega_0\right) + \psi\left(r, \varphi, z; \omega, \omega_0\right)\right]\right\rangle \approx \exp\left\{-\frac{2\pi^2}{c^2}\left[\omega_d^2 z \int_0^\infty \kappa \phi_{oc}(\kappa)\, \mathrm{d}\kappa + (\omega_0 + \omega_c)^2 r^2 z\left[1 - \cos\left(\varphi - \varphi'\right)\right] \int_0^\infty \kappa^3 \phi_{oc}(\kappa)\, \mathrm{d}\kappa\right]\right\}, \quad (12)$$

where $\omega_c = (\omega' + \omega)/2$, $\omega_d = \omega' - \omega$, $\phi_{oc}(\kappa)$ represents the spatial power spectrum of refraction-index fluctuations of asymmetric oceanic turbulence and is expressed as [39]

$$\phi_{oc}(\kappa) = \varepsilon^{-1/3}\beta A^2 \chi_T \frac{\left[1 + C_1\left(\kappa_{x,y}\eta\right)^{2/3}\right]}{4\pi\left(\kappa_{x,y}^2 + \kappa_0^2\right)^{11/6}} \left\{\exp\left[-\frac{\left(\kappa_{x,y}\eta\right)^2}{R_T^2}\right] + \frac{1}{\varpi^2\theta_S}\exp\left[-\frac{\left(\kappa_{x,y}\eta\right)^2}{R_S^2}\right] - \frac{1+\theta_S}{\varpi\theta_S} \times \exp\left[-\frac{\left(\kappa_{x,y}\eta\right)^2}{R_{TS}^2}\right]\right\}, 0 < \kappa < \infty, \quad (13)$$

where $\kappa_{x,y}^2 = [(\mu_x^2 + \mu_y^2) + (\mu_x^2 - \mu_y^2)\cos(2\theta)]\kappa^2/2$, μ_x and μ_y are the asymmetric factors in the x and y directions, $\theta = \arctan(\mu_y/\mu_x)$, $\kappa_0 = 1/L_0$, L_0 is outer scale, ε is the rate of dissipation of turbulent kinetic energy per unit mass of fluid, C_1 is a free parameter, β is the Obukhov–Corrsin constant, $G_i(\kappa) = \exp[-(\kappa\eta)^2/R_i^2]$, η is the inner scale of turbulence, $R_i = \frac{\sqrt{3}}{Q^{3/2}}(W_i - \frac{1}{3} + \frac{1}{9W_i})^{3/2}$, Q is the non-dimensional constant, $W_i = \{[(\frac{1}{27} - \frac{\mathrm{Pr}_i}{6\beta Q^{-2}})^2 - \frac{1}{729}]^{1/2} - (\frac{1}{27} - \frac{\mathrm{Pr}_i}{6\beta Q^{-2}})\}^{1/3}$, Pr_T and Pr_S respectively represents the Prandtl numbers of the temperature and salinity, $A = 2.6 \times 10^{-4}$liter/ deg, $\mathrm{Pr}_{TS} = 2\mathrm{Pr}_T\mathrm{Pr}_S/(\mathrm{Pr}_T + \mathrm{Pr}_S)$, χ_T is the rate of the dissipation of mean-squared temperature, $\varpi = A(dT_0/dz)/[B(dS_0/dz)]$ defines the contributions of the temperature and salinity distributions to the distribution of the refractive index, dT_0/dz and dS_0/dz are respectively the differences in temperature and salinity between the top and bottom boundaries of the domain under study, $\theta_S = K_T/K_S$ is the ratio of the eddy thermal diffusivity K_T to the diffusion of the salt K_S and is expressed as

$$\theta_S = \frac{|\varpi|}{R_F} \approx \begin{cases} 1/\left(1 - \sqrt{(|\varpi| - 1)/|\varpi|}\right) & |\varpi| \geq 1 \\ 1.85|\varpi| - 0.85 & 0.5 \leq |\varpi| \leq 1 \\ 0.15|\varpi| & |\varpi| \leq 0.5. \end{cases} \quad (14)$$

Substituting Eq. (13) into Eq. (12) and integrating over κ, and with the help of the integral expression at $\kappa_0^2/\kappa_m^2 \ll 1$ [42]

$$\int_0^\infty \kappa^{2\mu} \frac{\exp\left(-\kappa^2/\kappa_m^2\right)}{\left(\kappa_0^2 + \kappa^2\right)^{11/6}} d\kappa \approx \frac{1}{2}\kappa_0^{2\mu - 8/3}\Gamma\left(\mu + \frac{1}{2}\right)\left[\frac{\Gamma(4/3 - \mu)}{\Gamma(11/6)} + \frac{\Gamma(\mu - 4/3)}{\Gamma(\mu + 1/2)}\left(\frac{\kappa_0^2}{\kappa_m^2}\right)^{4/3-\mu}\right], \quad (15)$$

we derive the analytical expression of the complex phase perturbation of spatiotemporal waves as

$$\left\langle \exp\left[\psi^*\left(r, \varphi', z; \omega', \omega_0\right) + \psi\left(r, \varphi, z; \omega, \omega_0\right)\right]\right\rangle \approx \exp\left\{-\omega_d^2\Omega - (\omega_0 + \omega_c)^2\,\mu\right\}, \quad (16)$$

where

$$\Omega = \frac{\pi z}{8c^2}\beta A^2 \varepsilon^{-1/3}\chi_T \left\{\kappa_0^{-5/3}\left[1.2\left(1 + \frac{\varpi^{-2}}{\theta_S} - \frac{1+\theta_S}{\varpi\theta_S}\right) - 6.68\kappa_0^{5/3}\eta^{5/3}\left(R_T^{-5/3} + \frac{\varpi^{-2}}{\theta_S}R_S^{-5/3} - \frac{1+\theta_S}{\varpi\theta_S}R_{TS}^{-5/3}\right)\right] + 0.893C_1\eta^{2/3}\kappa_0^{-1}\left[1.88\left(1 + \frac{\varpi^{-2}}{\theta_S} - \frac{1+\theta_S}{\varpi\theta_S}\right) - 3.97\kappa_0\eta\left(R_T^{-1} + \frac{\varpi^{-2}}{\theta_S}R_S^{-1} - \frac{1+\theta_S}{\varpi\theta_S}R_{TS}^{-1}\right)\right]\right\}\Phi\left(\mu_x, \mu_y\right), \quad (17)$$

and

$$\mu = \frac{\pi r^2 z\beta A^2 \varepsilon^{-1/3}\chi_T}{8c^2}\left[1-\cos\left(\varphi-\varphi'\right)\right]\left\{\kappa_0^{1/3}\left[-7.2\left(\frac{\varpi^{-2}}{\theta_S}+1-\frac{1+\theta_S}{\varpi\theta_S}\right)\right.\right.$$
$$\left.+5.57(\kappa_0\eta)^{-1/3}\left(R_T^{1/3}+\frac{\varpi^{-2}}{\theta_S}R_S^{1/3}-\frac{1+\theta_S}{\varpi\theta_S}R_{TS}^{1/3}\right)\right]+1.19C_1\eta^{2/3}\kappa_0$$
$$\left.\times\left[-3.76\left(\frac{\varpi^{-2}}{\theta_S}+1-\frac{1+\theta_S}{\varpi\theta_S}\right)+1.49(\kappa_0\eta)^{-1}\left(R_T+\frac{\varpi^{-2}}{\theta_S}R_S-\frac{1+\theta_S}{\varpi\theta_S}R_{TS}\right)\right]\right\}\Phi\left(\mu_x,\mu_y\right), \tag{18}$$

where $\Phi(\mu_x,\mu_y)=\int_0^{2\pi}2[(\mu_x^2+\mu_y^2)+(\mu_x^2-\mu_y^2)\cos(2\theta)]^{-1}\mathrm{d}\theta$.

4. Probability Distribution of OAM Modes for Lommel-Gaussian Pulsed Beam

When the vortex pulsed beam propagates in the asymmetric oceanic turbulence, the refractive index fluctuation induces the phase aberrations that disturbs the complex amplitude of this beam and alters the original eigenstates of OAM. Consider a vortex pulsed beam that initially has a transverse spatial wave function and a temporal function, oceanic turbulence alters the pulse shape and the pulse width of the vortex pulsed beam propagation. In previous studies [38], we introduce a new OAM eigenfunctions with temporal factors to study the effects of oceanic turbulence on Laguerre-Gaussian pulsed beams based on the orthogonal basis expansion of Laguerre polynomial. However, Lommel-Gaussian pulsed beam essentially consists of the infinite linear superposition of Bessel modes whose wave vectors have identical axial projections. Utilizing the weighted orthogonal characteristic of Bessel function

$$\sum_P J_{m_0+2n}\left[\frac{(\omega+\omega_0)\,r}{c\sin^{-1}(\vartheta_0)}\right]J_{m_0+2n}\left[\frac{(\omega+\omega_0)\,r'}{c\sin^{-1}(\vartheta_0)}\right]\exp\left(-\frac{r^2+r'^2}{w_0^2}\right)=\frac{\delta(r,r')}{r}, \tag{19}$$

we construct the OAM eigenfunctions by the method in Ref. [34]

$$B_{P,m,t}(r,\varphi,\omega)=\frac{\sqrt{T_0}}{2\pi}J_{m_0+2n}\left[\frac{(\omega+\omega_0)\,r}{c}\sin(\vartheta_0)\right]\exp\left(-\frac{r^2}{w_0^2}\right)\exp\left(\mathrm{i}m\varphi+\mathrm{i}\omega t_0\right), \tag{20}$$

where $t_0=nT_0$.

In a single pulse cycle, Lommel-Gaussian pulsed beams $v(r,\varphi,z;\omega_0,\omega)$ propagate through oceanic turbulence as a superposition of eigenstates [13], [38]

$$v(r,\varphi,z;\omega,\omega_0)=\sum_P a_{P,m,t}(z,t)B_{P,m,t}(r,\varphi,\omega), \tag{21}$$

where $a_{P,m,t}(z,t)$ represents the superposition coefficients and t is continuous time within a half-pulse width. Then, we obtain the coefficients $a_{P,m,t}(z,t)$ using the basis projections as

$$a_{P,m,t}(z,t)=\frac{\sqrt{T_0}}{2\pi}\iiint J^*_{m_0+2n}\left[\frac{(\omega+\omega_0)\,r}{c\sin^{-1}(\vartheta_0)}\right]\exp\left(-\frac{r^2}{w_0^2}\right)\exp\left[-\mathrm{i}\left(m\varphi-\omega t\right)\right]v(r,\varphi,z;\omega,\omega_0)\,r\mathrm{d}r\mathrm{d}\varphi\mathrm{d}\omega. \tag{22}$$

We can sum the probabilities associated with eigenvalues to obtain the conditional probability as [13]

$$p(m\,|m_0,t)=\sum_P\left|a_{P,m,t}(z,t)\right|^2. \tag{23}$$

Substituting Eqs. (19) and (22) into Eq. (23) and then integrating over r', since oceanic turbulence causes the random aberrations, we can obtain the received probability by taking the ensemble

average as

$$p_a(m,t) = \langle p(m|m_0,t)\rangle = \frac{T_0}{(2\pi)^2}\iiint\iint S(\omega)\,S^*(\omega')\left\langle v_0^*(r,\varphi,z;\omega,\omega_0)\,v_0(r,\varphi',z;\omega',\omega_0)\right\rangle_{oc} \times \exp\left[\mathrm{i}(\omega-\omega')t - \mathrm{i}m(\varphi-\varphi')\right] r\mathrm{d}r\mathrm{d}\varphi\mathrm{d}\varphi'\mathrm{d}\omega\mathrm{d}\omega', \tag{24}$$

where $\langle\cdots\rangle_{oc}$ denotes the ensemble average of oceanic turbulence.

Substituting Eq. (4) into Eq. (24), the conditional probability can be expressed as

$$p_a(m,t) = T_0\iiint\left\langle W(r,\varphi,\varphi',z;t)\right\rangle \exp\left[-\mathrm{i}m(\varphi-\varphi')\right] r\mathrm{d}r\mathrm{d}\varphi\mathrm{d}\varphi', \tag{25}$$

where $\langle W(r,\varphi,\varphi',z;t)\rangle$ is the special coherence function and D is the receiver diameter.

The analytical expression of the special coherence function can be obtained as (see in Appendix A)

$$\begin{aligned}\left\langle W(r,\varphi,\varphi',z;t)\right\rangle = {} & \frac{E_0^2}{2\pi}\exp\left[-\frac{2z^2}{w_0^2}\left(\sin^2(\vartheta_0)+\frac{r^2}{z^2}\right)\right]\sum_{n=0}^{\infty}\left|\mathrm{I}_{m_0+2n}\left[\frac{\sin(\vartheta_0)\,2zr}{w_0^2}\right]\right|^2 \\ & \times\sum_{u=0}^{m_0+2n}\frac{(m_0+2n)!\,(2m_0+4n-2u)!}{(m_0+2n-u)!u!\sqrt{(T_0^2+2\mu)}}\exp\left(-\frac{\mu{\omega_0}^2T_0^2}{T_0^2+2\mu}\right)\left[\frac{w_0^2\omega_0T_0^2}{2zc(T_0^2+2\mu)}\right]^{2m_0+4n-u} \\ & \times\sum_{H=1}^{\lfloor m_0+2n-u\rfloor}\left(\frac{T_0^2+2\mu}{2\omega_0^2T_0^4}\right)^H\frac{2^{u+1}\left(T_0^2+8\Omega\right)^{-u/2-1/2}\left(T_0^2+2\mu\right)^u}{(2m_0+4n-2u-2H)!H!\omega_0^uT_0^{2u}} \\ & \times\exp\left(-\frac{\xi^2}{T_0^2+8\Omega}\right)D_u\left(\frac{\xi}{\sqrt{(T_0^2/4+2\Omega)}}\right)\exp\left[\mathrm{i}(m_0+2n)(\varphi-\varphi')\right]Q_1^{4n}.\end{aligned} \tag{26}$$

where $\lfloor n\rfloor$ is the integral part of the real number n, $D_u(\cdot)$represents the parabolic cylinder function, and $\xi = t-[1-\sin^2(\vartheta_0)/2]z/c$.

The received probability of OAM modes of the Lommel-Gaussian pulsed beams in the receiver plane is determined by integrating over r at the upper limit of the receiver diameter [38]

$$P(m,t) = \frac{P_D(m,m_0,\xi)}{\sum_{q=-\infty}^{\infty}P_D(q=m,m_0,\xi=0)}, \tag{27}$$

where

$$\begin{aligned}P_D(m,m_0,\xi) = {} & \frac{E_0^2}{2\pi}T_0\iint\int_0^{D/2}\exp\left[-\frac{2z^2}{w_0^2}\left(\sin^2(\vartheta_0)+\frac{r^2}{z^2}\right)\right]\sum_{n=0}^{\infty}\left|\mathrm{I}_{m_0+2n}\left[\frac{\sin(\vartheta_0)\,2zr}{w_0^2}\right]\right|^2 \\ & \times\sum_{u=0}^{m_0+2n}\frac{(m_0+2n)!\,(2m_0+4n-2u)!}{(m_0+2n-u)!u!\sqrt{(T_0^2+2\mu)}}\exp\left[\mathrm{i}2n(\varphi-\varphi')-\frac{\mu{\omega_0}^2T_0^2}{T_0^2+2\mu}\right]\left[\frac{w_0^2\omega_0T_0^2}{2zc(T_0^2+2\mu)}\right]^{2m_0+4n-u} \\ & \times\sum_{H=1}^{\lfloor m_0+2n-u\rfloor}\left(\frac{T_0^2+2\mu}{2\omega_0^2T_0^4}\right)^H\frac{2^{u+1}\left(T_0^2+8\Omega\right)^{-u/2-1/2}\left(T_0^2+2\mu\right)^u}{(2m_0+4n-2u-2H)!H!\omega_0^uT_0^{2u}} \\ & \times D_u\left(\xi/\sqrt{(T_0^2/4+2\Omega)}\right)\exp\left[-\xi^2/\left(T_0^2+8\Omega\right)\right]Q_1^{4n}\exp\left[\mathrm{i}(m_0-m)(\varphi-\varphi')\right]r\mathrm{d}r\mathrm{d}\varphi\mathrm{d}\varphi',\end{aligned} \tag{28}$$

where D represents the receiver diameter, $P_D(m,m_0,\xi)$ represents the received probability of signal OAM modes when the OAM quantum number in oceanic turbulence m is equal to the initial OAM quantum number m_0,$P_D(m,m_0,\xi)$ represents the received probability of crosstalk OAM modes when the OAM quantum number in oceanic turbulence m is not equal to the initial OAM quantum number

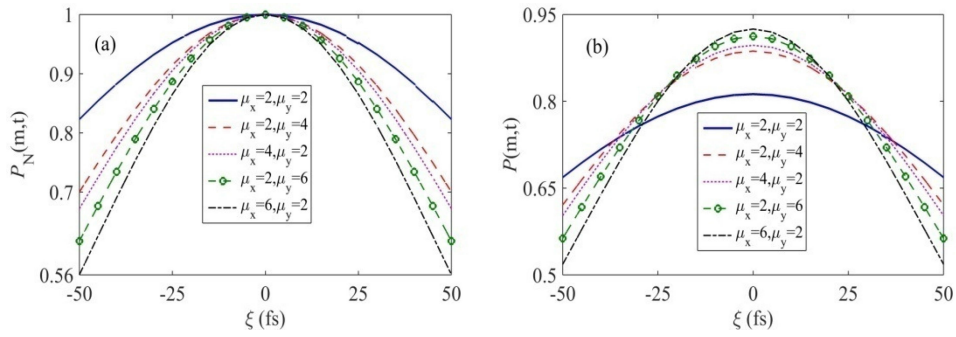

Fig. 2. (a) Normalized probability $P_N(m, t)$ (b) probability $P(m, t)$ of signal OAM modes versus co-moving coordinate $\xi = t - [1 - \sin^2(\vartheta_0)/2]z/c$ for different the asymmetric factors in the x-direction μ_x and in the y-direction μ_y.

$m_0, \sum_{q=-\infty}^{\infty} P_D(q = m, m_0, \xi = 0)$ represents the sum of all the received probability of OAM modes for a given initial OAM quantum number m_0.

To analyze the pulse broadening during the vortex pulsed beam propagation in oceanic turbulence, we define the normalized probability $P_N(m, t)$ of the signal OAM modes as

$$P_N(m, t) = \frac{P_j(m, t)}{\max\left[P_1(m, t), \ldots, P_j(m, t), \ldots, P_M(m, t)\right]} \tag{29}$$

where the subscript parameter M represents a natural number, the subscript parameter j represents an arbitrary natural number from 1 to M, $P_j(m, t)$ represents an received probability of OAM modes $P(m, t)$ in arbitrary modes.

5. Numerical Simulation and Analysis

We analyze and discuss the numerical simulation of the Lommel-Gaussian pulsed with OAM propagating in asymmetric oceanic turbulence. In the numerical simulation, except for the special parameters, the parameters are given as follows: $z = 150$ m, $m = 1$, $m_0 = 1$, $w_0 = 5$ cm, $\vartheta_0 = 0.001$, $T_0 = 20$ fs, $\mu_x = 2$, $\mu_y = 3$, $D = 5$ cm, $\varepsilon = 10^{-3}\mathrm{m}^2/\mathrm{s}^3$, $\eta = 1$ mm, $\lambda = 532$ nm, $\varpi = -0.45$ and $\chi_T = 10^{-8}\mathrm{K}^2/\mathrm{s}$.

According to the relation between the pulse broadening and the bandwidth ($\Delta\omega = 2\pi/\Delta\tau$), the pulse broadening must be known to obtain high bandwidths for high-power optical communication and avoid pulse–pulse interference for Lommel-Gaussian pulsed beams. We know that the pulse broadening can be described by the full width half maximum value (FWHM) of the pulse profile [43]. In order to objectively describe the pulse broadening during pulse transmission in oceanic turbulence, we normalize the peak value of probability distribution of the signal OAM modes to one. In following discussion, we use the absolute difference between two co-moving coordinate values when the normalized probability of OAM mode reaches a half of its maximum as the pulse width.

In Fig. 2, we calculate the normalized probability $P_N(m, t)$ and the probability $P(m, t)$ of OAM signal modes for Lommel-Gaussian pulsed beam propagation as a function of the co-moving coordinate $\xi = t - [1 - \sin^2(\vartheta_0)/2]z/c$ and the asymmetric factors of oceanic turbulence in the x-direction μ_x and in the y-direction μ_y. Form Fig. 2, the peak values of the probability of OAM signal modes always appear at the mean arrival time $\xi = 0$ as the co-moving coordinate $\xi = t - [1 - \sin^2(\vartheta_0)/2]z/c$ changes. In other words, there is hardly any the pulse delay in such cases. In addition, Fig. 2(a) shows that the pulse broadening decreases with increasing asymmetric factors in the x-direction μ_x and in the y-direction μ_y. Fig. 2(b) shows the probability of signal OAM modes at $\xi = 0$ increasing with increasing of the asymmetric factors in the x-direction μ_x and in the y-direction μ_y. The phenomenon comes from that the asymmetric factors in x and y directions improve the optical wireless system performance. The asymmetric factor of oceanic turbulence reduces the turbulence

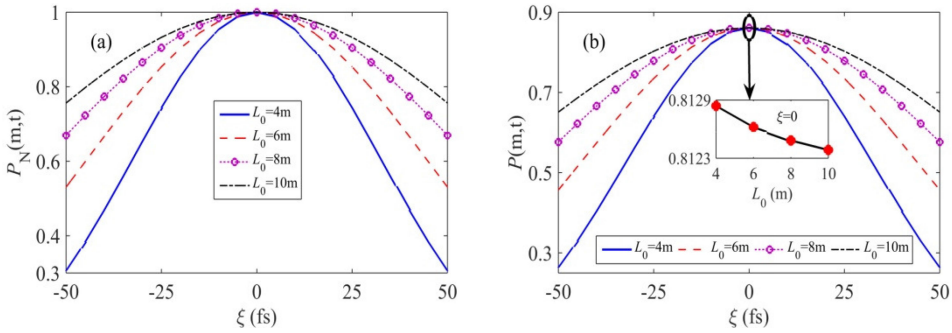

Fig. 3. (a) Normalized probability $P_N(m, t)$ (b) probability $P(m, t)$ of signal OAM modes versus co-moving coordinate $\xi = t - [1 - \sin^2(\vartheta_0)/2]z/c$ for different the outer scale of oceanic turbulence L_0.

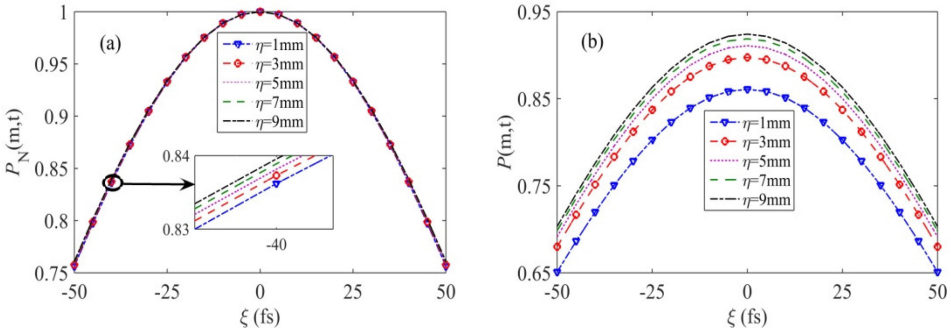

Fig. 4. (a) Normalized probability $P_N(m, t)$ (b) probability $P(m, t)$ of OAM signal modes versus co-moving coordinate $\xi = t - [1 - \sin^2(\vartheta_0)/2]z/c$ for different the inner scale η.

interference on the received probability of signal OAM modes and the pulse broadening. Thus, the propagation of beam through the communication channels with large asymmetric factor of oceanic turbulence can achieve a good quality of UWOC.

To comprehend the influence of oceanic turbulent parameters on the pulse broadening and the received probability of signal OAM modes, Fig. 3 shows that the normalized probability $P_N(m, t)$ and the probability $P(m, t)$ of signal OAM modes for Lommel-Gaussian pulsed beam versus co-moving coordinate ξ for different the outer scale of oceanic turbulence L_0. Fig. 3(a) shows that the pulse broadening increases with the outer scale of oceanic turbulence L_0 increasing. In addition, from Fig. 3(b), the received probability of signal OAM modes slightly decreases with the increasing of the outer scale of oceanic turbulence L_0. The larger outer scale of oceanic turbulence L_0 causes a large light refraction and a large scintillation level at the diffractive beam edge, which results in a larger temporal broadening and a small received probability of signal OAM modes. Thus, the pulsed beam propagating in the communication channel with a small outer scale can realize the much information capacity and high-power transmission in asymmetric oceanic turbulence.

We also study the influence of the inner scale η on the normalized probability $P_N(m, t)$ and the probability $P(m, t)$of signal OAM modes for Lommel-Gaussian pulsed beams propagating in oceanic turbulence. Fig. 4(a) shows that the pulse broadening has a very small increase with increasing inner scale η. The reason for this phenomenon is that the inner scale of turbulence mainly causes the optical scattering. But the pulse broadening is sensitive to the optical refractions rather than the optical scattering. The effect of inner scale on the pulse broadening can be neglected because the inner scale causes a very small refraction. From Fig. 4(b), we can see that, as the inner scale of oceanic turbulence η increases, the received probability of signal OAM modes of Lommel-Gaussian pulsed beam increases. Duo to large inner scale of turbulent eddy corresponding to a small light

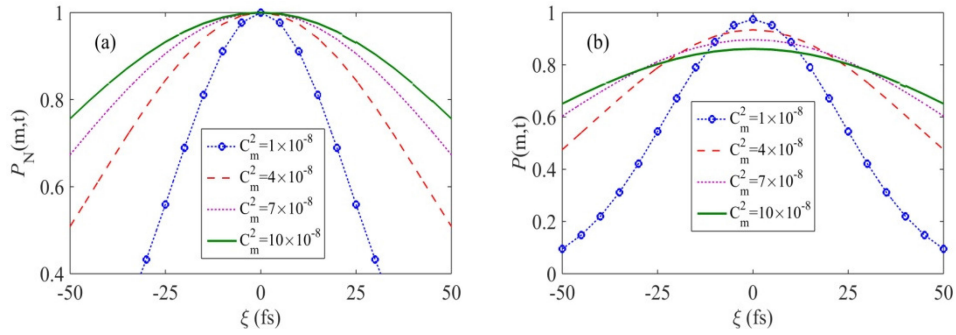

Fig. 5. (a) Normalized probability $P_N(m, t)$, (b) probability $P(m, t)$ of signal OAM modes versus co-moving coordinate $\xi = t - [1 - \sin^2(\vartheta_0)/2]z/c$ for different the temperature structure constant C_m^2.

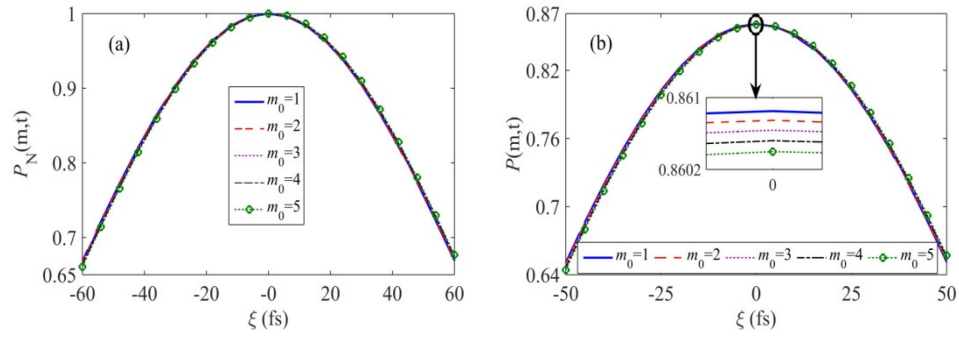

Fig. 6. (a) Normalized probability $P_N(m, t)$ (b) probability $P(m, t)$ of OAM signal modes versus co-moving coordinate $\xi = t - [1 - \sin^2(\vartheta_0)/2]z/c$ for different OAM quantum number m_0.

scattering and inducing the small energy loss, the greater inner scale of oceanic turbulence causes a larger value of the received probability of signal OAM modes. Thus, the vortex pulsed beam propagating through oceanic turbulent channel with a large inner scale causes a low energy loss, which can improve the quality of UWOC.

In Fig. 5, we calculate the normalized probability and the received probability of the signal OAM mode versus the co-moving coordinate $\xi = t - [1 - \sin^2(\vartheta_0)/2]z/c$ and the temperature structure constant $C_m^2 = \varepsilon^{-1/3}\chi_t$. It is evident from Fig. 5(a) that the pulse broadening increases with increasing the temperature structure constant C_m^2. This is caused by the large temperature structure constant C_m^2 corresponding to a strong oceanic turbulence which results in a strong temporal broadening. In addition, Fig. 5(b) shows that the peak value of the received probability of the signal OAM modes at $\xi = 0$ decreases with increasing the temperature structure constant C_m^2. The phenomenon can be explained that a large temperature structure constant C_m^2 corresponds to a strong oceanic turbulence causing the large attenuation of signal.

To further comprehend the influence of light source parameters of Lommel-Gaussian pulsed beams on the pulse broadening and the received probability of signal OAM modes. Figs. 6(a) and (b) depict the normalized probability and the probability of OAM signal modes as a function of the co-moving coordinate $\xi = t - [1 - \sin^2(\vartheta_0)/2]z/c$ for different OAM quantum number m_0. Fig. 6(a) shows that the pulse broadening has a weak dependence on the OAM quantum number. This result indicates that the turbulence aberration has the same effect on the temporal broadening for different OAM modes. As would be expected, the received probability of the signal OAM modes decreases with increasing the OAM quantum number m_0 in Fig. 6(b), but the reduction of the

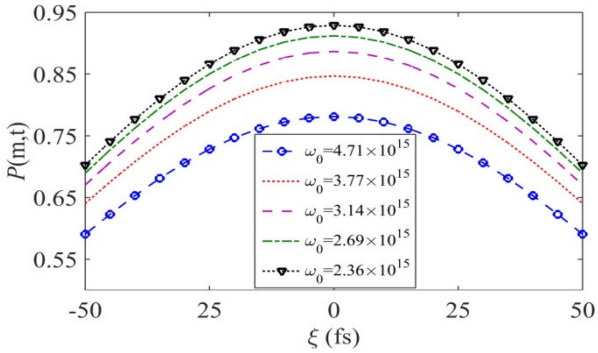

Fig. 7. Probability of signal OAM modes $P(m, t)$ versus co-moving coordinate $\xi = t - [1 - \sin^2(\vartheta_0)/2]z/c$ for different the carrier frequency ω_0.

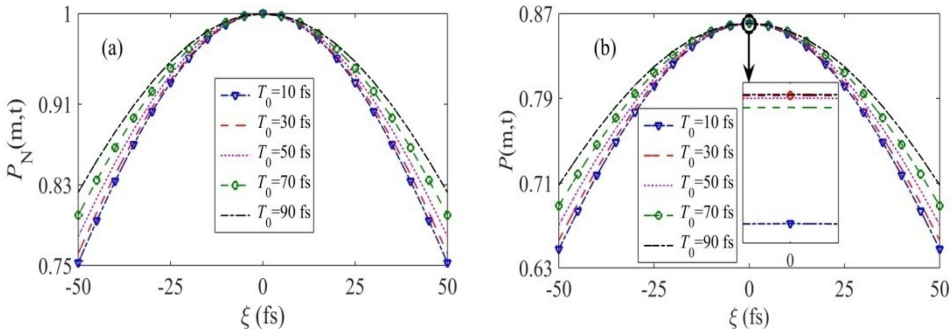

Fig. 8. (a) Normalized probability $P_N(m, t)$ (b) probability $P(m, t)$ of OAM signal modes versus co-moving coordinate $\xi = t - [1 - \sin^2(\vartheta_0)/2]z/c$ for different initial half-pulse width T_0.

received probability of the signal OAM modes is very small. These results reveal that Lommel-Gaussian pulsed beam has a good anti-turbulence interference characteristic when it carries more information capacity.

In Fig. 7, we further investigate the received probability of signal OAM modes of Lommel-Gaussian pulsed beam as functions of the carrier frequency ω_0 and the co-moving coordinate $\xi = t - [1 - \sin^2(\vartheta_0)/2]z/c$ in the UWOC channel. Fig. 7 shows the received probability of signal OAM modes decreasing with increasing of the carrier frequency ω_0. The result reveals that Lommel-Gaussian pulsed beam with a large carrier frequency ω_0 is more affected by oceanic turbulence. In addition, we find that the pulse broadening is independent of the carrier frequency ω_0 and do not show the changes of the pulse broadening in this article for non-redundant.

Fig. 8 further illuminates the influence of initial half-pulse width on the normalized probability and the received probability of signal OAM modes. As would be expected, Fig. 8(a) shows that the pulse broadening has a strong dependence on the initial half-pulse width T_0. In Fig. 8(b), the received probability of signal OAM modes increases with increasing of the initial half-pulse width T_0. In the mean arrival time $\xi = 0$, the initial half-pulse width T_0 causes a weak influence on the probability of signal OAM modes. This phenomenon can be explained that a large initial half-pulse width results in a small temporal scintillation [44].

We derive the complex phase perturbation of spatiotemporal wave in this paper that includes the spatial and temporal effects of oceanic turbulence on Lommel-Gaussian pulsed beams propagation. Thus, we compare the received probabilities of Lommel-Gaussian pulsed beams and Lommel-Gaussian continuous beams in oceanic turbulence. Fig. 9 depicts that the continuous Lommel-Gaussian beams (Non-pulse) obtain a larger probability of OAM signal modes ($|m - m_0| = 0$) and a

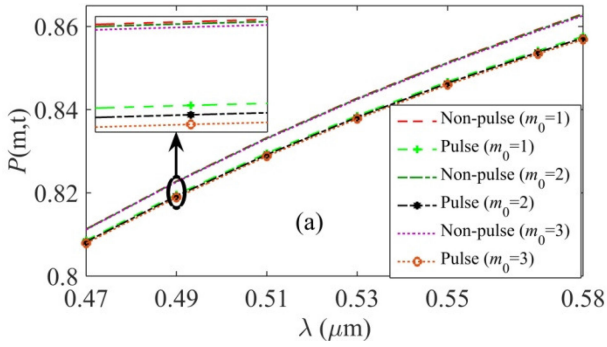

Fig. 9. Probability $P(m, t)$ of OAM signal modes versus wavelength λ for different OAM quantum number m_0.

smaller probability of OAM crosstalk modes ($|m - m_0| = 1$) than Lommel-Gaussian pulsed beams (Pulse). This result is derived from the additional temporal scintillation of pulsed beams caused by oceanic turbulence. But the continuous beams do not have the temporal scintillation. As the wavelength λ decreases, the probabilities of OAM signal modes and OAM crosstalk modes for continuous Lommel-Gaussian beams are closer to that for Lommel-Gaussian pulsed beams. This phenomenon can be explained that the short wavelength λ corresponds to a high frequency and a strong laser emission power. The pulsed beams for high-power laser emission have better resistance to the temporal scintillation caused by oceanic turbulence than the pulsed beams for low-power laser emission. In addition, experimental results demonstrate that the most suitable optical wavelength for underwater optical communication is in the region of blue and green window. That is to say, we can choose the Lommel-Gaussian pulsed beams to solve the small-scale self-focusing limiting the system performance and efficiency of high-power laser propagation in oceanic turbulence.

6. Conclusions

In this paper, we focused on the influence of asymmetric oceanic turbulence on the pulse broadening and the received probability of the OAM modes carried by Lommel-Gaussian pulsed beams. We derived an analytical expression of the complex phase perturbation of spatiotemporal wave that contains the outer scale and the asymmetric factors of oceanic turbulence. Based on the OAM eigenfunctions of the series of Bessel modes, the normalized probability model and the probability model of signal OAM modes for Lommel-Gaussian pulsed beams propagation through asymmetric oceanic turbulence were established. Our results show that Lommel-Gaussian pulsed beams realize high data rate transmission in the weak oceanic turbulence with a small outer scale and a large asymmetric factor. In addition, the large received probability of signal OAM modes in UWOC can be obtained when Lommel-Gaussian pulsed beam with a large carrier frequency propagates in the weak asymmetric oceanic turbulence with a small outer scale, which realizes the high information capacity transmission. Lommel-Gaussian pulsed beam carrying large OAM quantum number has a good anti-turbulence interference characteristic and carries more information capacity. Our theoretical model and results can improve the performance and efficiency of high-power laser propagation in UWOC channel by Lommel-Gaussian pulsed beams carrying information.

Acknowledgment

The authors wish to thank the anonymous reviewers for their valuable suggestions.

Appendix A

Substituting Eq. (3) into Eq. (5), the two-frequency MCF of the continuous Lommel-Gaussian beam in the absence of turbulence is given as

$$\Gamma_2^0\left(r,\varphi,\varphi',z;\omega,\omega'\right)=\exp\left[\mathrm{i}\left(\varphi-\varphi'\right)\left(m_0+2n\right)\right]\frac{E_0^2\left(\omega_0+\omega\right)\left(\omega_0+\omega'\right)w_0^4}{4z^2c^2\sqrt{1+z_{\xi,1}^2}\sqrt{1+z_{\xi,2}^2}}\exp\left[\left(\omega-\omega'\right)\frac{\mathrm{i}}{c}\left(z+\frac{r^2}{2z}\right)\right]$$
$$\times\exp\left\{-\frac{w_0^2}{4c^2}\left[\frac{\left(\omega_0+\omega\right)^2}{1-\mathrm{i}z_{\xi,1}}+\frac{\left(\omega_0+\omega'\right)^2}{1+\mathrm{i}z_{\xi,2}}\right]\left[\sin^2\left(\vartheta_0\right)+\frac{r^2}{z^2}\right]\right\}\sum_{n=0}^{\infty}Q^{4n}\left|\mathrm{I}_{m_0+2n}\left\{\frac{w_0^2\sin\left(\vartheta_0\right)r\left(\omega_0+\omega'\right)^2}{\left[2zc^2\left(1+\mathrm{i}z_{\xi,2}\right)\right]}\right\}\right|^2, \tag{A1}$$

where $z_{\xi,1}=\left(\omega_0+\omega\right)\frac{w_0^2}{2zc}$ and $z_{\xi,2}=\left(\omega_0+\omega'\right)\frac{w_0^2}{2zc}$.

Making use of the sum frequency $\omega_c=\left(\omega+\omega'\right)/2$ and difference frequency $\omega_d=\omega-\omega'$, under the near-field assumption $z_R\gg z$, the two-frequency MCF of the continuous Lommel-Gaussian beam in the absence of turbulence is simplified as

$$\Gamma_2^0\left(r,\varphi,\varphi',z;\omega_d,\omega_c\right)=E_0^2\exp\left[-\frac{2z^2}{w_0^2}\left(\sin^2\left(\vartheta_0\right)+\frac{r^2}{z^2}\right)\right]\exp\left[\omega_d\frac{\mathrm{i}z}{c}\left(1-\frac{\sin^2\left(\vartheta_0\right)}{2}\right)\right]$$
$$\times\sum_{n=0}^{\infty}\exp\left[\mathrm{i}\left(m_0+2n\right)\left(\varphi-\varphi'\right)\right]Q_1^{4n}\left|\mathrm{I}_{m_0+2n}\left[\frac{\sin\left(\vartheta_0\right)2zr}{w_0^2}\right]\right|^2\left[\frac{w_0^4}{\left(2zc\right)^2}\left(\omega_0+\omega_c\right)^2+i\frac{\omega_d w_0^2}{2zc}\right]^{m_0+2n}. \tag{A2}$$

In addition, we can obtain a special product form of the Fourier transform of the amplitude of the Gaussian pulse

$$S\left(\omega\right)S^*\left(\omega'\right)=\pi T_0^2\exp\left[-\frac{1}{4}\left(\omega^2+\omega'^2\right)T_0^2\right]=\pi T_0^2\exp\left(-\frac{1}{2}\omega_c^2T_0^2\right)\exp\left(-\frac{1}{8}\omega_d^2T_0^2\right). \tag{A3}$$

Then, substituting Eqs. (A2), (A3) and (16) into Eq. (4), we rewrite the special coherence function as

$$\left\langle W\left(r,\varphi,\varphi',z;t\right)\right\rangle=\frac{E_0^2}{4\pi^2}\exp\left[-\frac{2z^2}{w_0^2}\left(\sin^2\left(\vartheta_0\right)+\frac{r^2}{z^2}\right)\right]\sum_{n=0}^{\infty}Q_1^{4n}\left|\mathrm{I}_{m_0+2n}\left[\frac{\sin\left(\vartheta_0\right)2zr}{w_0^2}\right]\right|^2$$
$$\times\exp\left[\mathrm{i}\left(m_0+2n\right)\left(\varphi-\varphi'\right)\right]\int\int_{-\infty}^{+\infty}\exp\left(-\frac{1}{2}\omega_c^2T_0^2\right)\left[\frac{w_0^4}{\left(2zc\right)^2}\left(\omega_0+\omega_c\right)^2+i\frac{\omega_d w_0^2}{2zc}\right]^{m_0+2n}$$
$$\times\exp\left(-\frac{1}{8}\omega_d^2T_0^2-\mathrm{i}\omega_dt\right)\exp\left[\omega_d\frac{\mathrm{i}z}{c}\left(1-\frac{\sin^2\left(\vartheta_0\right)}{2}\right)\right]\exp\left[-\omega_d^2\Omega-\left(\omega_0+\omega_c\right)^2\mu\right]\mathrm{d}\omega_c\mathrm{d}\omega_d. \tag{A4}$$

Making use of the following mathematical formula $\left(x+y\right)^m=\sum_{u=0}^{m}\frac{m!}{(m-u)!u!}x^{m-u}y^u$, we obtain an expanded formula for the convenience of integration in Eq. (A4) as

$$\left[\frac{w_0^4}{\left(2zc\right)^2}\left(\omega_0+\omega_c\right)^2+i\frac{\omega_d w_0^2}{2zc}\right]^{m_0+2n}=\sum_{u=0}^{m_0+2n}\frac{\left(m_0+2n\right)!(i\omega_d)^u}{\left(m_0+2n-u\right)!u!}\left[\frac{w_0^2}{2zc}\left(\omega_0+\omega_c\right)\right]^{2m_0+4n-u}. \tag{A5}$$

Substituting Eq. (A5) into Eq. (A4) and integrating over $\omega_c + \omega_0$ and ω_d, and with the help of the integral expressions [42]

$$\int_{-\infty}^{+\infty} x^n \mathrm{e}^{-px^2+2qx}\mathrm{d}x = n!\mathrm{e}^{q^2/p}\sqrt{\frac{\pi}{p}}\left(\frac{q}{p}\right)^n \sum_{H=1}^{\lfloor n/2 \rfloor} \frac{1}{(n-2H)!H!}\left(\frac{p}{4q^2}\right)^k \quad [p>0] \tag{A6}$$

$$\int_{-\infty}^{+\infty} (ix)^n \exp\left(-p^2x^2 - iqx\right)\mathrm{d}x = 2^{-n/2}\sqrt{\pi}\,p^{-n-1}\exp\left(-\frac{q^2}{8p^2}\right) D_n\left(\frac{q}{\sqrt{2}p}\right), \tag{A7}$$

the analytic expression of the special coherence function for Lommel-Gaussian pulsed beam in Eq. (26) can be obtained.

References

[1] H. Zhang and Y. Dong, "General stochastic channel model and performance evaluation for underwater wireless optical links," *IEEE Trans. Wireless Commun.*, vol. 15, no. 2, pp. 1162–1173, Feb. 2016.

[2] Y. Huang, B. Zhang, Z. Gao, G. Zhao, and Z. Duan, "Evolution behavior of Gaussian Schell model vortex beams propagating through oceanic turbulence," *Opt. Express*, vol. 22, no. 15, pp. 17723–17734, Jul. 2014.

[3] M. V. Jamali, F. Akhoundi, and J. A. Salehi, "Performance characterization of relay-assisted wireless optical CDMA networks in turbulent underwater channel," *IEEE Trans. Wireless Commun.*, vol. 15, no. 6, pp. 4104–4116, Jun. 2016.

[4] D. Zou, C. Gong, and Z. Xu, "Signal detection under short-interval sampling of continuous waveforms for optical wireless scattering communication," *IEEE Trans. Wireless Commun.*, vol. 17, no. 5, pp. 3431–3443, May 2018.

[5] Y. Li, L. Yu, and Y. Zhang, "Influence of anisotropic turbulence on the orbital angular momentum modes of Hermite-Gaussian vortex beam in the ocean," *Opt. Express*, vol. 25, no. 11, pp. 12203–12215, May 2017.

[6] X. Cui *et al.*, "Analysis of an adaptive orbital angular momentum shift keying decoder based on machine learning under oceanic turbulence channels," *Opt. Commun.*, vol. 429, no. 15, pp. 57–62, Dec. 2018.

[7] A. E. Willner *et al.*, "Underwater optical communications using orbital angular momentum-based spatial division multiplexing," *Opt. Commun.*, vol. 408, no. 1, pp. 21–25, Feb. 2018.

[8] Y. Zhang, L. Shan, Y. Li, and L. Yu, "Effects of moderate to strong turbulence on the Hankel-Bessel-Gaussian pulse beam with orbital angular momentum in the marine atmosphere," *Opt. Express*, vol. 25, no. 11, pp. 33469–33479, Dec. 2017.

[9] M. Cheng, L. Guo, J. Li, and Y. Zhang, "Channel capacity of the OAM based free-space optical communication links with Bessel–Gauss beams in turbulent ocean," *IEEE Photon. J.*, vol. 8, no. 1, Feb. 2016, Art. no. 7901411.

[10] L. Allen, M. Beijersbergen, R. Spreeuw, and J. Woerdman, "Orbital angular momentum of light and the transformation of Laguerre–Gaussian laser modes," *Phys. Rev. A*, vol. 45, pp. 8185–8189, Jun. 1992.

[11] G. Molina-Terriza, J. P. Torres, and L. Torner, "Management of the angular momentum of light: preparation of photons in multidimensional vector states of angular momentum," *Phys. Rev. Lett.*, vol. 88, Dec. 2001, Art. no. 13601.

[12] M. Cheng, L. Guo, J. Li, Q. Huang, Q. Cheng, and D. Zhang, Propagation of an optical vortex carried by a partially coherent Laguerre–Gaussian beam in turbulent ocean, *Appl. Opt.*, vol. 55, no. 17, pp. 4642–4648, Jun. 2016.

[13] C. Paterson, "Atmospheric turbulence and orbital angular momentum of single photons for optical communication," *Phys. Rev. Lett.*, vol. 94, no. 15, Apr. 2005, Art. no. 153901.

[14] V. V. Nikishov and V. I. Nikishov, "Spectrum of turbulent fluctuations of the sea-water refraction index," *Int. J. Fluid Mech. Res.*, vol. 27, no. 1, pp. 82–98, 2000.

[15] X. Yi and I. B. Djordjevic, "Power spectrum of refractive-index fluctuations in turbulent ocean and its effect on optical scintillation," *Opt. Express*, vol. 26, no. 8, pp. 10188–10202, Apr. 2018.

[16] W. Lu, L. Liu, and J. F. Sun, "Influence of temperature and salinity fluctuations on propagation behaviour of partially coherent beams in oceanic turbulence," *J. Opt. A. Pure Appl. Opt.*, vol. 8, no. 12, pp. 1052–1058, Nov. 2006.

[17] J. Yao, Y. Zhang, R. Wang, Y. Wang, and X. Wang, "Practical approximation of the oceanic refractive index spectrum," *Opt. Express*, vol. 25, no. 19, pp. 23283–23292, Sep. 2017.

[18] M. Jamali *et al.*, "Statistical studies of fading in underwater wireless optical channels in the presence of air bubble, temperature, and salinity random variations (long version)," *IEEE Trans. Commun.*, vol. 66, no. 10, pp. 4706–4723, Oct. 2018.

[19] M. Cheng, L. Guo, J. Li, X. Yan, R. Sun, and Y. You, "Effects of asymmetry atmospheric eddies on spreading and wander of Bessel–Gaussian Beams in anisotropic turbulence," *IEEE Photon. J.*, vol. 10, no. 4, Aug. 2018, Art. no. 6100510.

[20] W. Wang, Z. Wu, Q. Shang, and L. Bai, "Propagation of Bessel Gaussian beams through non-Kolmogorov turbulence based on Rytov theory," *Opt. Express*, vol. 26, no. 17, pp. 21712–21724, Aug. 2018.

[21] Y. Zhu, X. Liu, J. Gao, Y. Zhang, and F. Zhao, "Probability density of the orbital angular momentum mode of Hankel-Bessel beams in an atmospheric turbulence," *Opt. Express*, vol. 22, no. 7, pp. 7765–7772, Mar. 2014.

[22] Y. Jin *et al.*, "Beam wander of a partially coherent Airy beam in oceanic turbulence," *J. Opt. Soc. Amer. A*, vol. 35, no. 8, pp. 1457–1464, Aug. 2018.

[23] Y. Yuan, D. Liu, Z. Zhou, H. Xu, J. Qu, and Y. Cai, "Optimization of the probability of orbital angular momentum for Laguerre-Gaussian beam in Kolmogorov and non-Kolmogorov turbulence," *Opt. Express*, vol. 26, no. 17, pp. 21861–21871, Aug. 2018.

[24] A. A. Kovalev and V. V. Kotlyar, "Lommel modes," *Opt. Commun.*, vol. 338, no. 1, pp. 117–122, Mar. 2015.

[25] L. Yu and Y. Zhang, "Analysis of modal crosstalk for communication in turbulent ocean using Lommel-Gaussian beam," *Opt. Express*, vol. 25, no. 19, pp. 22565–22574, Sep. 2017.
[26] D. E. Kelly and L. C. Andrews, "Temporal broadening and scintillations of ultrashort optical pulse," *Wave Random Complex*, vol. 9, no. 3, pp. 307–325, 1999.
[27] J. Eggert, B. Bourdon, S. Nolte, J. Rischmueller, and M. Imlau, "Chirp control of femtosecond-pulse scattering from drag-reducing surface-relief gratings," *Photon. Res.*, vol. 6, no. 6, pp. 542–548, Jun. 2018.
[28] C. Y. Young, L. C. Andrews, and A. Ishimaru, "Time-of-arrival fluctuations of a space–time Gaussian pulse in weak optical turbulence: an analytic solution," *Appl. Opt.*, vol. 37, no. 33, pp. 7655–7660, Nov. 1998.
[29] D. H. Froula *et al.*, "Spatiotemporal control of laser intensity," *Nature Photon.*, vol. 12, pp. 262–265, May 2018.
[30] C. Chen, H. Yang, S. Tong, B. Ren, and Y. Li, "Characterization of temporal pulse broadening for horizontal propagation in strong anisotropic atmospheric turbulence," *Opt. Express*, vol. 23, no. 4, pp. 4814–4828, Feb. 2015.
[31] A. J.-Navas, J. M. G.-Balsells, M. C.-Vázquez, and A. P. Notario, "Numerical model for the temporal broadening of optical pulses propagating through weak atmospheric turbulence," *Opt. Lett.*, vol. 34, no. 23, pp. 3662–366, Dec. 2009.
[32] Ó. M.-Matos, P. Vaveliuk, J. Izquierdo, and V. Loriot, "Femtosecond spatial pulse shaping at the focal plane," *Opt. Express*, vol. 21, no. 21, pp. 25010–25025, Oct. 2013.
[33] J. Nie, G. Liu, and R. Zhang, "Propagation and spatiotemporal coupling characteristics of ultra-short gaussian vortex pulse," *Opt. Laser Technol.*, vol. 101, pp. 446–450, May 2018.
[34] Y Liu and C. Gao, "Study on the time-varying and propagating characteristics of ultrashort pulse Laguerre-Gaussian beam," *Opt. Express*, vol. 18, no. 12, pp. 12104–12110, May 2010.
[35] V. A. Banakh and L. O. Gerasimova, "Strong scintillations of pulsed Laguerrian beams in a turbulent atmosphere," *Opt. Express*, vol. 24, no. 17, pp. 19264–19277, Aug. 2016.
[36] F. Ye, J. Zhang, J. Xie, and D. Deng, "Propagation properties of the rotating elliptical chirped Gaussian vortex beam in the oceanic turbulence," *Opt. Commun.*, vol. 426, pp. 456–462, Nov. 2018.
[37] Y. Li, Y. Zhang, and Y. Zhu, "Influence of oceanic turbulence on propagation of the Gaussian pulsed X wave carrying orbital angular momentum," *Opt. Commun.*, vol. 428, pp. 57–62, Jul. 2018.
[38] Y. Li, Y. Zhang, and Y. Zhu, "Probability distribution of the orbital angular momentum mode of the ultrashort Laguerre-Gaussian pulsed beam propagation in oceanic turbulence," *Results Phys.*, vol. 11, pp. 698–705, Oct. 2018.
[39] Y. Li, Y. Zhang, and Y. Zhu, "Oceanic spectrum of unstable stratification turbulence with outer scale and scintillation index of Gaussian-beam wave" *Opt. Express*, vol. 27, no. 5, pp. 7656–7672, Mar. 2019.
[40] L. C. Andrews and R. L. Phillips, *Laser Beam Propagation Through Random Media*. Washington, DC: SPIE, 2005.
[41] T. Shirai, A. Dogariu, and E. Wolf, "Mode analysis of spreading of partially coherent beams propagating through atmospheric turbulence" *J. Opt. Soc. Amer. A*, vol. 20, no. 6, pp. 1094–1102, Jun. 2003.
[42] I. S. Gradshteyn and I. M. Ryzhiz, *Table of Integrals, Series and Products*. New York, NY, USA: Academic Press, 2006.
[43] M. Ornigotti, C. Conti, and A. Szameit, "Effect of orbital angular momentum on nondiffracting ultrashort optical pulses," *Phys. Rev. Lett.*, vol. 115, Sep. 2015, Art. no. 100401.
[44] D. Kelly and L.C. Andrews, "Temporal broadening and scintillations of ultrashort optical pulses," *Waves Random Media*, vol. 9, no. 3, pp. 307–325, 1999.